

---

---

MOLECULAR  
BIOPHYSICS

---

---

# Functionalization of Amino Modified Probes for Atomic Force Microscopy

A. Limanskii

*Institute of Microbiology and Immunology, Ukrainian Academy of Medical Sciences,  
Pushkinskaya ul., 14, Kharkov, 61057, Ukraine  
Laboratory of Plasma Membrane and Nuclear Signaling, Graduate School of Biostudies,  
Kyoto University, Kyoto, 606-8502, Japan.  
E-mail: o.lymunskiy@mail.ru*

Received August 26, 2005

**Abstract**—The probes for atomic force microscopy (AFM) functionalized by bovine serum albumin (BSA) were obtained; they can be used for molecular recognition studies. The procedure of modification and functionalization of the AFM probe included three stages. First, amino probes were obtained by modification in vapors of amino silane derivative. Then, a covalent bond was formed between the surface amino groups of the probe and a homobifunctional amino reactive crosslinker. Finally, the probe with a covalently attached crosslinker was functionalized by BSA molecules. The AFM probes were characterized by force measurements at different stages of the modification; the adhesion force and the work of adhesion force were determined. The modification process was confirmed by visualization of BSA and supercoiled pGEMEX DNA molecules immobilized on the standard amino mica and on amino mica modified by a crosslinker.

DOI: 10.1134/S0006350906020059

*Key words:* force measurements, atomic force microscopy, AFM, probe functionalization, homobifunctional crosslinker, recognition force spectroscopy

## INTRODUCTION

Atomic force microscopy (AFM) was used to obtain high-resolution images of DNA, proteins, cells, and cell organelles [1–5]. AFM was also successfully applied for direct determination of the forces required to separate the molecular complexes formed by the molecules adsorbed on the surfaces of the AFM probe and substrate. This field of AFM, which enables direct measurement of the forces of interaction between molecular pairs, was initially termed chemical force microscopy; it is presently known as single molecule recognition force microscopy and is a powerful tool for research at the molecular level [6–10]. Immobilization

of the molecules on the surface of an AFM probe is the key moment in such research.

Functionalization of AFM probes by biomolecules (primarily by proteins) makes it possible to study the micromechanical characteristics of molecules, macromolecules, and the cell—the forces that keep proteins within cell membranes. In the case of probes with immobilized antibodies or other specific receptors, localization of various proteins, polysaccharides, and messenger RNA within both the cell and the cell nucleus can be achieved with nanometer resolution. For example, since mRNA localization in different zones of the cytoplasm is an important element of posttranscriptional control, a method for investigating gene expression in single animal cells without damaging them seriously was developed [11]. The mRNA molecules were extracted from the cell

---

**Abbreviations:** AFM, atomic force microscopy; BSA, bovine serum albumin; PEG, polyethylene glycol; APTES, 3-aminopropyltriethoxy silane; DSS, disuccinimidyl suberate; EGS, ethylene glycol-*bis*-(*N*-hydroxysuccinimide ester of succinic acid).



and ethylene glycol-*bis*-(*N*-hydroxysuccinimide ester of succinic acid) (EGS linker, Sigma, Japan). Bovine serum albumin (BSA) was used for the subsequent immobilization. The process of functionalization was performed in a commercial fluid AFM cell and consisted of the following stages. The amino probes were mounted in a glass cell, the DSS linker solution ( $2.7 \cdot 10^{-3}$  M in 0.5% triethylamine/chloroform) was injected, and the probes were incubated for 15 min. The cell was then washed thoroughly with 200  $\mu$ l of PBS buffer, and the force plots were recorded for the system consisting of the amino probe functionalized with linker and mica (with which the DSS linker can also interact). The substrate was then replaced with freshly cleaved mica, and force measurements were repeated. For BSA immobilization, BSA solution was injected into the fluid cell and incubated for 5 min; the cell was then washed with PBS buffer, the substrate was changed with freshly cleaved mica and a series of force curves was recorded for the probe with immobilized BSA.

**Preparation of DNA and BSA samples for AFM.** Supercoiled pGEMEX1 DNA (3993 bp) from Promega (United States) and bovine serum albumin (the 5th fraction; Pierce, United States) were used in experiments. Amino mica or linker-functionalized amino mica were used as substrates. A 10- $\mu$ l drop of BSA solution (0.001–0.02 g/ml in PBS buffer) or of DNA solution (0.1–1.0 g/ml in TE buffer) was placed on a 1 cm<sup>2</sup> strip of amino mica and incubated for 2 min. The strip was then washed with deionized water, blown with argon, and incubated for 20 min under a pressure of 100 mm Hg.

**Force measurements.** All the measurements were performed using a Nanoscope IV MultiMode System atomic force microscope (Veeco Instruments Inc., United States), equipped with a E-scanner and a commercial fluid cell. The tip deflection–*Z* position graphs (tip deflection depending on the distance between the tip and the mica surfaces, further termed the force distance plots) were recorded at a vertical scanning frequency of 1 Hz and a *Z* amplitude of 50–200 nm. The force–distance plots were obtained from the tip deflection–*Z* position dependence (i.e., the scanner position along the *Z* axis) by the Nanoscope software package (version 5.12r3, Veeco Instruments Inc., United States). Most of the force plots were recorded at a 100-nm amplitude; for this amplitude, the rate of approximation and removal of tip and

mica surfaces was 200 nm/s. By multiplying this value by the effective spring constant of the probe, the loading rates of 2.6 and 5 nN/s were calculated for the cantilevers with the length of 200 and 100  $\mu$ m, respectively.

The force plots were recorded in the conventional force-calibration plot mode. The averages of 50–196 force plots for different variants of AFM probe modification were used to obtain the values of the adhesion force and the work of adhesion force. A total of 855 force curves were recorded and analyzed in this work. The data for 512 points were recorded for every cycle of force measurements (probe extending to and retracting from the substrate). All force measurements were performed with triangular (V-shaped) OMCL-TR400PSA cantilevers made of silicon nitride and covered with gold and a thin chromium layer (Olympus Optical Co., Japan). Each chip contained two long and two short cantilevers with different geometric sizes and, therefore, with different spring constants. The resonant frequencies of the cantilevers were determined using the built-in option of measuring the cantilever frequency in air (without taking into account a possible shift in the resonant frequency caused by air damping).

The spring constant for each cantilever was determined by Cleveland's resonant frequency method. The value of the rigidity constant is proportional to the cube of the resonant frequency for an unloaded cantilever [16]:

$$K = 2 \cdot \rho \cdot l^3 \cdot \sqrt{\frac{3}{E}} \cdot \omega_0^3, \quad (1)$$

where  $K$  is the spring constant;  $E$ , the modulus of elasticity;  $\omega_0$ , the measured resonant frequency;  $\rho$ , the density of the composite material of the cantilever; and  $h_1$  and  $l$ , the width and length of the cantilever, respectively.

The modulus of elasticity and the density of the cantilever should be known in order to determine  $K$  by Cleveland's method. The modulus of elasticity of the composite cantilever was determined from the proportion [17]

$$E_{\text{cant}} = \frac{h_1 E_{\text{SiN}} + h_2 E_{\text{Au}} + h_3 E_{\text{Cr}}}{h_1 + h_2 + h_3}, \quad (2)$$

where  $E_{\text{SiN}} = 197$  and  $214$  GPa for the 100 and 200  $\mu$ m cantilevers, respectively;  $E_{\text{Au}} = 81$  GPa;  $E_{\text{Cr}} = 288.1$  GPa;  $h_1 + h_2 + h_3$  is the total thickness of the

cantilever; and  $h_1$ ,  $h_2$ , and  $h_3$  are the thicknesses of  $\text{Si}_3\text{N}_4$ , Au, and Cr, respectively. The calculated values of the modulus of elasticity  $E_{\text{SiN}}$  were 197.2 and 182.5 GPa for the long and short cantilever, respectively.

In order to obtain reliable parameters of surface ionization from the results of AFM measurements, the quality of material is essential, due to the zwitterionic nature of silicon nitride surface.

Depending on the conditions of manufacturing of cantilevers, their stoichiometry and density may vary within a broad range. We used the value of silicon nitride density  $\rho_{\text{SiN}} = 2.8 \text{ g/cm}^3$ , corresponding to the stoichiometry N : Si = 1.1 [17];  $\rho_{\text{Au}} = 19.6 \text{ g/cm}^3$ , and  $\rho_{\text{Cr}} = 7.2 \text{ g/cm}^3$ . The value of effective density of the composite material of the  $\text{Si}_3\text{N}_4$ -Au-Cr cantilever was calculated from the proportion [17]:

$$\rho_{\text{cant}} = \frac{\rho_{\text{SiN}} h_1 + \rho_{\text{Au}} h_2 + \rho_{\text{Cr}} h_3}{h_1 + h_2 + h_3} \quad (3)$$

According to the manufacturer's information, for the OMCL-TR400PSA cantilevers, the thickness of SiN was  $h_{\text{SiN}} = 400 \text{ nm}$ , the thickness of the Cr layer  $h_{\text{Cr}} = 3 \text{ nm}$ , and the thickness of the gold layer  $h_{\text{Au}} = 60 \text{ nm}$ .

The density of the V-shaped composite cantilevers used in this study was  $\rho = 5.00 \text{ g/cm}^3$ .

The following buffer solutions were used for the measurements: 10 mM Tris-HCl, pH 7.6; 1 mM EDTA (TE buffer); 137 mM NaCl; 2.7 mM KCl; 10 mM  $\text{Na}_2\text{HPO}_4$ ; 2 mM  $\text{KH}_2\text{PO}_4$ ; and PBS buffer (pH 7.4).

For force measurements, 200- $\mu\text{m}$  cantilevers with the resonant frequency in air  $f = 9\text{--}10 \text{ kHz}$  were usually applied. For statistical analysis of the values of adhesion force and the work of adhesion force, the Origin software package (version 5, United States) was used.

**Atomic force microscopy.** The AFM images of DNA and BSA were captured at room temperature by the tapping AFM in air in the height mode. The imaging was performed with OMCL-AC 160 TS cantilevers (Olympus Optical Co., Japan) with a tip resonant frequency of 340–360 kHz and nominal spring constant of 42 N/m, at a scan line frequency of 3 Hz. Simultaneously with the height and deflection signals, 512  $\times$  512 pixels images were acquired and processed

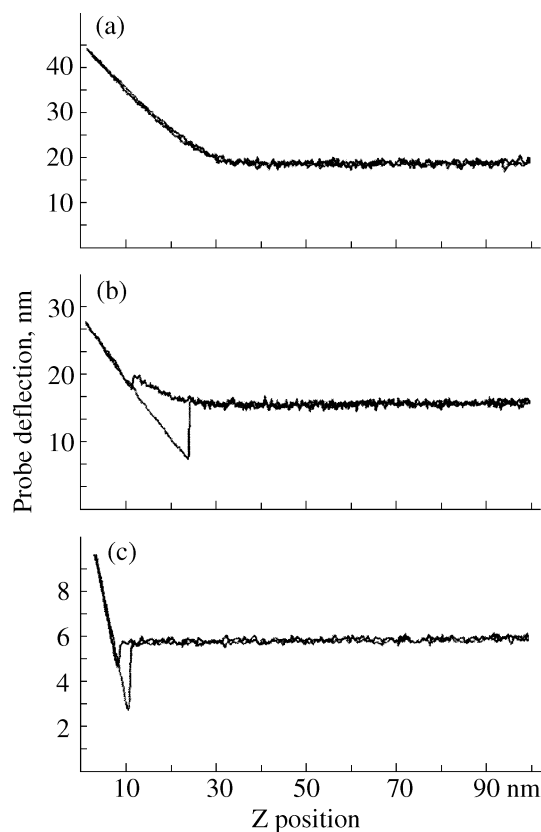


**Fig. 1.** Force plots (AFM probe deflection from the scanner position) for (a) unmodified and (b, c) amino modified probes. Notations: (a, b), cantilever length 200  $\mu\text{m}$ ; TE buffer; (c), cantilever length 100  $\mu\text{m}$ ; TE buffer, 1 M NaCl.

by flattening using the Nanoscope software package (version 5.12r3, Veeco Instruments Inc., USA).

## RESULTS AND DISCUSSION

Individual calibration of the cantilevers that are used for quantitative measurements is necessary due to substantial variation of the rigidity constant values for commercial cantilevers. The rigidity constants calculated from the proportion (1) were  $K = 0.025 \text{ N/m}$  for the long ( $l = 200 \text{ }\mu\text{m}$ ) cantilever and  $K = 0.008 \text{ N/m}$  for the short one ( $l = 100 \text{ }\mu\text{m}$ ).

The information concerning the adhesive properties (elasticity, rigidity) and the total charge of the interacting surfaces can be derived from the force graphs (two graphs are obtained in a cycle, one for the probe approximation to the surface and the other one for the probe removal). Figure 1a presents the characteristic force graphs for an unmodified probe recorded in TE buffer. It can be seen that the graphs of probe approximation and removal nearly coincide. Freshly

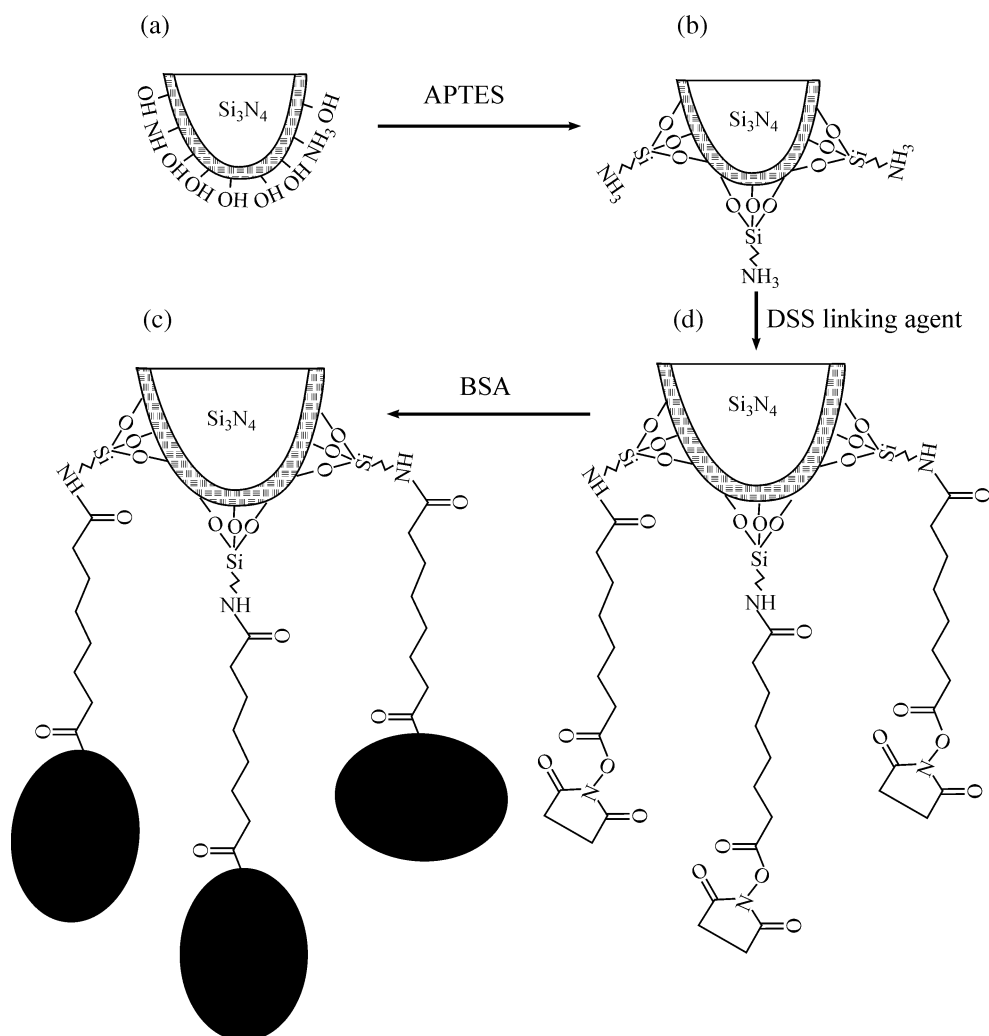


**Fig. 2.** Functionalization of AFM probes. (a) Unmodified silicon nitride AFM probe and (b) AFM probe with amino groups covering its surface. At the first stage, the probe surface becomes modified with covalently bound amino groups after treatment with the vapors of an amino silane derivative (APTES). (c) Probe with the DSS linker attached; free amino reactive ends contain NHS esters. During the second stage, the probe amino groups react with the NHS ester groups of the homobifunctional DSS linking agent. (d) Probe with BSA molecules covalently attached. The amino reactive groups of the DSS linking agent interact with the BSA lysine residues.

cleaved mica was used as the substrate. The characteristic bend in the left part of the graph and the absence of the so-called "probe jump into contact" indicate the same charge of the probe and substrate surfaces under these conditions. The total charge of the unmodified probe is negative, since mica is known to be negatively charged at neutral pH [18]. In spite of the presence of endogenous amino groups on the probe surface (according to the results of [13],  $\sim 640 \text{ } 120 \text{ per m}^2$ ), these results confirm the similarity between the surface properties of mica and the silicon nitride probe, as the oxidized surfaces of both mica and the probe are covered with OH groups. This is the reason for which visualization of BSA and

pGEMEX DNA immobilized on the modified mica was used to develop the procedure of functionalization and characterization of the modified surface. The AFM images of protein and pGEMEX DNA served as additional controls of probe surface modification and provided supplementary data for interpretation of the force graphs.

The characteristic toothlike peak can be seen on the graph of removal of the amino probe with the surface coating of protonated amino groups. The adhesion force can be determined from the maximal value of the peak; the work of adhesion force, from its area. The adhesion force and the work of adhesion force characterize the quality of probe modification; they

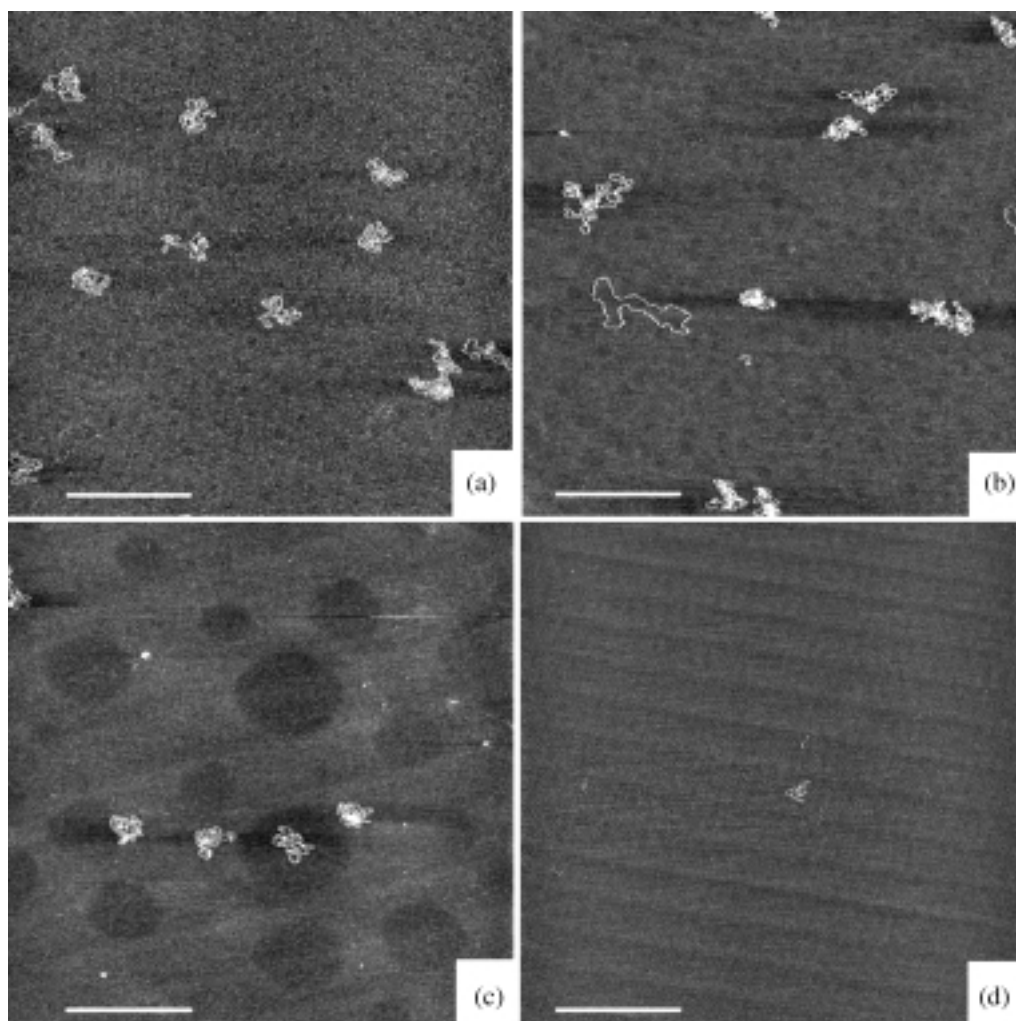


**Fig. 3.** AFM images of supercoiled pGEMEX DNA (3993 bp) immobilized on different substrates. (a) Amino mica. Picture area,  $2 \times 2 \mu\text{m}$ . (b) Amino mica treated with 0.5% triethylamine in chloroform for 15 min. Picture area,  $2 \times 2 \mu\text{m}$ . Scale bar, 500 nm. (c) Amino mica treated with 0.5% triethylamine in chloroform for 30 min. Picture area,  $2 \times 2 \mu\text{m}$ . Scale bar, 500 nm. (d) Amino mica functionalized by the EGS homobifunctional linking agent (treated with EGS solution in 0.5% triethylamine/chloroform for 5 min). Picture area,  $4 \times 4 \mu\text{m}$ . Scale bar, 1  $\mu\text{m}$ .

show the force of breaking-off and the work of adhesion force required to disrupt the contact between the probe and substrate surfaces. The value of adhesion force for the amino probe in TE buffer determined from the force graph was  $F = 103 \text{ pN}$ . Screening of positively charged amino groups in a solution of high ionic strength (Fig. 1c;  $I = 1 \text{ M Na}^+$ ) resulted in a decrease of the adhesion force to 93 pN; the adhesive effect, however, persisted. This relationship between the ionic strength and adhesion force is in good agreement with the previously obtained results for gold-covered V-shaped cantilevers with higher rigidity constants [15].

The general scheme of probe modification and subsequent functionalization is shown in Fig. 2. The

density of molecules on the tip surface is an important probe characteristic of single molecule recognition force microscopy. A modified probe with a single receptor molecule for specific binding with the substrate is the ideal case. The fact that the APTES molecule interacts with three OH groups on the probe surface is a characteristic feature of probe amino modification by APTES (Fig. 2b). Therefore, the number of amino groups on the surface of the probe treated with APTES must be significantly less than in the case of a probe treated using some other procedure, e.g., with ethanolamine and subsequent formation of self-associated monolayers. The number of amino groups on the surface of the ethanolamine-treated probe was shown to be 1.5-fold higher than in the case of gas phase modification by APTES [13]. Accepting that

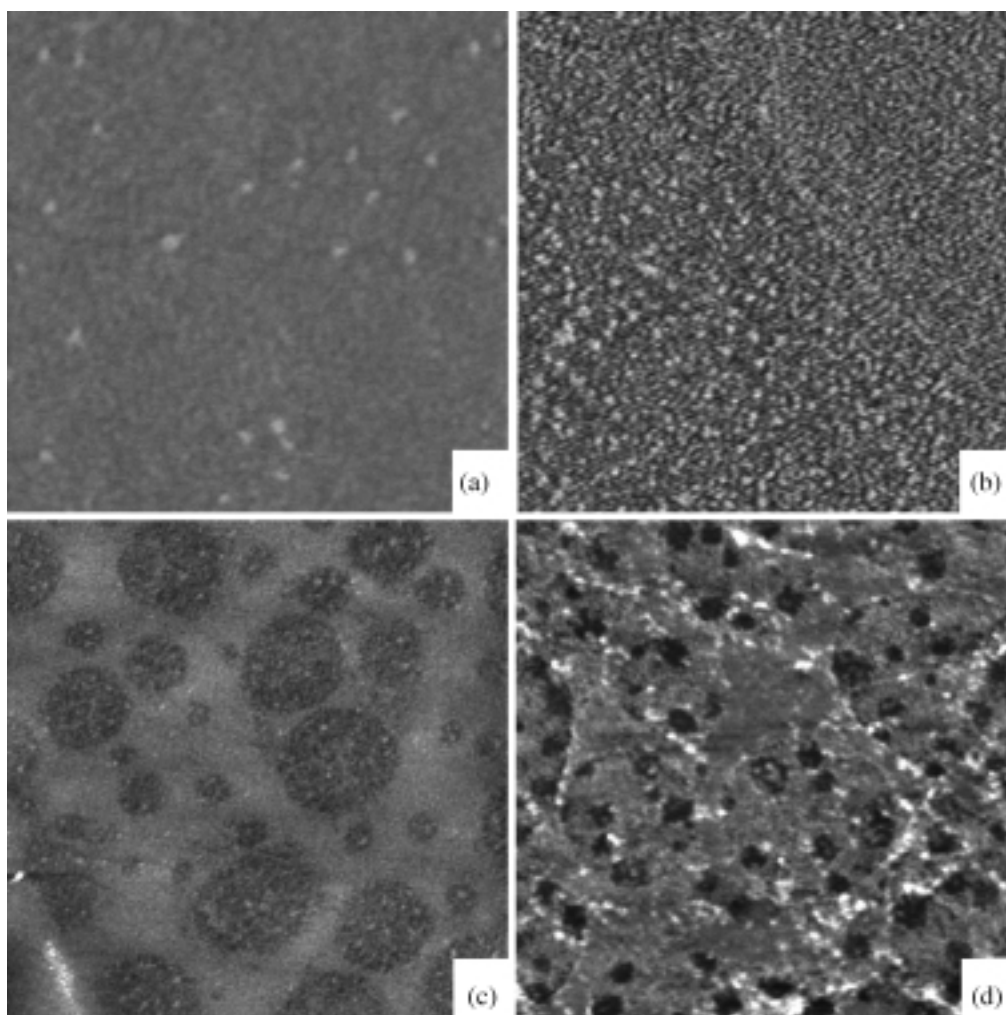


**Fig. 4.** AFM images of bovine serum albumin immobilized on amino mica treated with different reagents. (a) BSA on amino mica obtained by treatment with APTES vapors. Picture area,  $700 \times 700$  nm. (b) BSA on amino mica treated with 0.5% triethylamine in chloroform for 15 min. Picture area,  $2 \times 2$   $\mu$ m. (c) BSA on amino mica treated with 0.5% triethylamine in chloroform for 30 min. Picture area,  $2 \times 2$   $\mu$ m. (d) BSA on amino mica functionalized by EGS homobifunctional linking agent (treated by EGS solution in 0.5% triethylamine/chloroform for 5 min). Picture area,  $4 \times 4$   $\mu$ m.

the number of amino groups on APTES-treated surface is  $1730 \pm 200$  per  $\text{m}^2$  [13], we get as many as 27 amino groups on the side surface (i.e., on the hemispherical surface) for a tip with the radius  $R = 50$  nm. In the case of a sharpened tip with a radius of  $R = 13$  nm [19, 20], only two amino groups will be exposed on its side surface. The fact that only 50% of amino groups are active (protonated) should be also taken into account.

The application of homobifunctional amino-reactive linking agents (e.g., DCC) is also intended to decrease the number of receptor molecules on the probe surface. Only one variant is shown in Fig. 2c, namely, the variant with one end of the linker (NHS ether) interacting with the amino group of the probe,

while the amino groups of lysine residues in BSA can interact with the other, free end of the linker. However, both NHS ends of the linker can bind to the amino groups of the probe, thereby decreasing the number of free amino groups on the probe surface.

The linker molecules must meet certain requirements: they must (i) have a certain length, (ii) be soluble in solvents used for complex formation with biomolecules, and (iii) their elasticity must be predictable [9].

In the course of preliminary experiments, 0.5% triethylamine solution in chloroform (vol/vol) was chosen as the solvent for both linking agents; the results obtained with the use of another solvent, dimethyl sulfoxide, are not shown. The amino

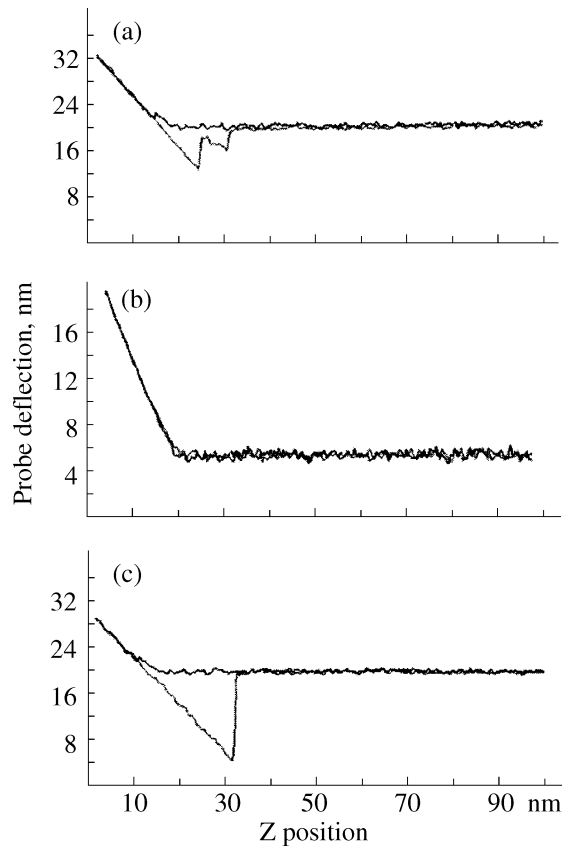


**Fig. 5.** Force plots for the amino modified probe (a) at different stages of functionalization with a homobifunctional DSS linking agent and (b, c) immobilization of BSA. (a) Measurements were performed on freshly cleaved mica. (b, c) Force plots after amino probe modification with the DSS linker and BSA immobilization, respectively. Freshly cleaved mica was used for the measurements after BSA immobilization. Plots (a, c) were recorded in the course of modification of the same cantilever. All measurements were performed in PBS buffer.

modified mica was treated with the EGS linking agent dissolved in this solvent. The effect of the duration of treatment on the adsorption characteristics of the amino modified mica is shown in Fig. 3. The force plots for the amino modified mica–probe pair of surfaces were previously shown to be both qualitatively and quantitatively similar to the plots for the amino probe–mica pair [22]. The results for the amino mica can therefore be extrapolated to the amino probes. Together with the shape of supercoiled pGEMEX DNA molecules, their number per unit area reflects the number of protonated amino groups involved in electrostatic interaction with the phosphate groups in DNA; i.e., it can be considered a specific criterion of amino mica quality. Upon transition from the standard amino modified mica (11–12 pGEMEX DNA

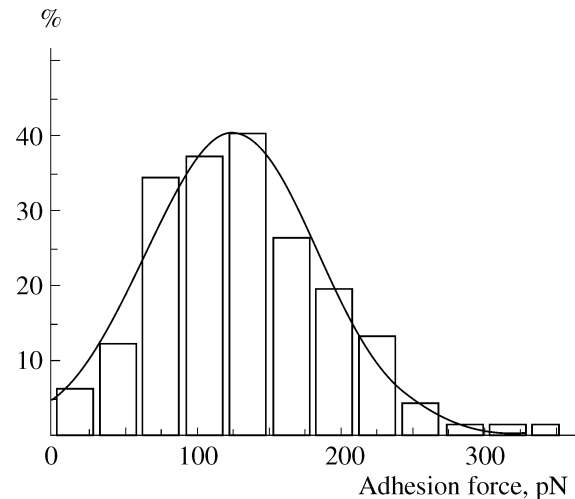


**Fig. 6.** The histogram of adhesion force for an amino modified probe with BSA covalently bound via the DSS linker. The adhesion force measured only after the last stage of probe functionalization with BSA is  $F = 26.9 \pm 7.2$  pN; the line represents the normal distribution.

molecules per  $4 \mu\text{m}^2$ , Fig. 3a), the number of DNA molecules immobilized on the amino mica decreased to 10–11 (15-min treatment with 0.5% triethylamine in chloroform, Fig. 3b) and to 4 molecules (30 min treatment, Fig. 5c). These results demonstrated that the number of DNA molecules immobilized on the amino mica surface did not decrease if the treatment duration  $t$  did not exceed 15 min. Moreover, the plectonomic configuration of pGEMEX DNA molecules was retained even at  $t = 30$  min. Thus, the number of amino groups on the surface of amino mica after short-term exposure ( $t = 15$  min) in 0.5% triethylamine/chloroform remained practically the same as on the surface of untreated amino mica.

Functionalization of amino mica with the EGS linking agent leads to a sharp decrease in the number of amino groups on its surface. For instance, as seen in Fig. 3d, only one pGEMEX DNA molecule was immobilized on an area of  $16 \mu\text{m}^2$ , i.e., on the area that is greater by a factor of 4 than the picture area in Figs. 3a–3c. DNA molecules are not adsorbed on the functionalized mica after 15 or 30 min of treatment with the EGS linking agent. Two types of interaction between the amino mica and the EGS linker are possible. First, both the amine-reactive ends of the linking agent can bind to the amino mica, thereby decreasing the number of free amino groups on the mica surface. Second, the linking agent can be bound to the amino mica with one NHS ester end; the other



Adhesion force and the work of adhesion force for the amino probes with a cantilever length of  $l = 200 \text{ nm}$ , which were modified by the DSS linker with subsequent functionalization by bovine serum albumin in PBS buffer.

No.	Modified probe	Adhesion force, $F$ , pN	Work of adhesion force, $W$ , pJ
1	Amino probe (TE buffer)	103 23	580 190
2	Amino probe (1 M NaCl) $l = 100 \text{ nm}$	93 15	251 71
3	Amino probe + DSS linker–mica + DSS linker	44 15	107 43
4	Amino probe + DSS linker–freshly cleaved mica	93 21	450 160
5	Amino probe + DSS linker + BSA	27 7	62 17

amine-reactive end remains free and can subsequently interact with the DNA substrate.

AFM images of bovine serum albumin immobilized on different substrates were captured in order to determine the mechanism of binding of the EGS linking agent with the amino mica. It can be seen that BSA binds equally well with the amino mica (Fig. 4a), with the amino mica treated with 0.5% triethylamine in chloroform for 15 (Fig. 4b) or 30 min (Fig. 4c) and, most importantly, with the mica functionalized by the EGS linking agent (Fig. 4d). The  $\alpha$ -amino groups of the N-terminus of protein molecules can interact with NHS esters; their number, however, is insignificant. The reactions with the side chains of amino acids are therefore important. Of the five amino acids containing nitrogen in their side chains, only the amino group of lysine interacts with NHS esters to yield a stable product (owing to formation of the covalent amide bond), with the release of *N*-hydroxysuccinimide.

The results of visualization of the supercoiled pGEMEX DNA (Fig. 3) and bovine serum albumin (Fig. 4) on the amino mica functionalized by an aminoreactive EGS linking agent indicate: (i) the interaction between the amino mica and the EGS linker and (ii) the interaction between BSA and EGS linker used to functionalize amino mica. These results provided a rationale for the functionalization of amino probes by the DSS linker, another amine-reactive agent.

The force plots for the interacting surfaces of the probe and the substrate after probe modification and functionalization with BSA are shown in Fig. 5. The force plots for the probe modified with the DSS linking agent are presented in Fig. 5a. Figures 5 b and 5c show the plots for the DSS-modified probe after BSA immobilization, as recorded for two different

cantilevers. The adhesion force for the probe modified with the DSS linker was calculated from the histogram of the adhesion force distribution; it was  $F = 93 \pm 20 \text{ pN}$  in PBS buffer. The shape of the force plots and the decrease in the adhesion force compared to the amino probes ( $F = 103 \pm 23 \text{ pN}$  in TE buffer) indicated the interaction between the DSS linker and the amino probe surface.

The values of adhesion force and the work of adhesion force for the different variants of amino probe modification and functionalization calculated from the histograms (one of these histograms is shown in Fig. 6) are summarized in the table. Freshly cleaved mica was used as a substrate; in the case of probe modification with the DSS linker, force plots were taken both for the freshly cleaved mica and for the mica modified with the DSS linker. Since amino probe modification was performed in a fluid AFM cell, force curves were recorded both for the substrate used for modification (designated in the table as mica + DSS linker) and for the freshly cleaved mica as a substrate. It can be seen from the comparison of the adhesion force values and the work of adhesion force for these two variants (rows 3 and 4 in the table) that both mica and the amino probe were modified by the DSS linker. Since the adhesion force was calculated from the maximal force value on the plot and the work of adhesion force was determined from the area limited by the force plot, the value of the adhesion force work provides more precise information on the nature of interacting surfaces. For example, the adhesion force values are equal for the amino probe (row 2 in the table) and for the amino probe modified by DSS linker (row 4 in the table). However, the work of adhesion force is more than four times higher for the amino probe modified by the DSS linker. This result indicates the qualitative differences between the surface of the amino probe and that of the amino probe +

DSS linker; a considerably greater force is required to separate the surfaces of mica and amino probe + DSS linker than for the mica—amino probe pair.

The decreased adhesion force for the BSA-modified probe ( $F = 27 \pm 7$  pN, Fig. 6) in comparison to the probe modified by the DSS linker confirms qualitatively and quantitatively the results concerning BSA interaction with mica functionalized with an amino-reactive EGS linker (Fig. 4d).

Thus, in this work, the modification scheme was presented and modification with subsequent functionalization by BSA was performed for the probes for atomic force microscopy. The probes with a covalently bound amine-reactive homobifunctional linker DSS and BSA were characterized by means of force measurements; the adhesion force values and the work of adhesion force were determined for each stage of modification and for the probe with attached BSA alone. Unlike the earlier modification schemes with constant surface charge density [12, 13, 15, 23], the technology of amino modification of probes in APTES vapors developed in this work enables fabrication of surfaces with a regulated amino group density. We suggest that the amino probes with a decreased surface charge density can be used to minimize the number of interacting protonated amino groups in the course of further probe modification and functionalization. This, in turn, will make it possible to decrease the number of protein molecules attached to the probe surface.

#### ACKNOWLEDGMENTS

Thanks are due to O. Limanskaya (Institute of Experimental and Clinical Veterinary Medicine, Ukraine Academy of Agricultural Sciences) for helpful discussions and critical remarks during the preparation of this paper.

The study was supported in part by the Japanese Society for the Promotion of Science (Japan) and a grant of the Academy of Medical Sciences of Ukraine.

#### REFERENCES

1. A. E. Pelling, Y. Li, W. Shi, and J. K. Gimzewski, *Proc. Natl. Acad. Sci. USA* **102** (18), 6484–6489 (2005).

2. S. B. Larson, Y. G. Kuznetsov, J. Day, et al., *Acta Crystallogr. Ser. D: Biol. Crystallogr.* **61** Part 4, 416–422 (2005).
3. C. C. Conwell, I. D. Vilfan, and N. V. Hud, *Proc. Natl. Acad. Sci. USA* **100** (16), 9296–9301 (2003).
4. D. C. G. Klein, C. M. Stroh, H. Jwnsenius, et al., *Chemphyschem.* **4**, 1367–1371 (2003).
5. T. Yamada, H. Arakawa, T. Okajima, et al., *Ultramicroscopy* **91**, 261–268 (2002).
6. M. Blank, T. Mai, J. Gibert, et al., *Proc. Natl. Acad. Sci. USA* **100** (20), 11357–11360 (2003).
7. W. Baumgartner, P. Hinterdorfer, and H. Schindler, *Ultramicroscopy* **82**, 85–95 (2000).
8. T. Okajima, H. Arakawa, M. T. Alam, et al., *Biophys. Chemistry* **107**, 51–61 (2004).
9. M. Kudera, C. Eschbaumer, H. Gaub, and U. Schubert, *Advanced Functional Materials* **13** (8), 615–620 (2003).
10. C. Friedsam, A. Becares, U. Jonas, et al., *Chem. Phys. Chem.*, No. 5, 388–393 (2004).
11. H. Uehara, T. Osada, and A. Ikai, *Ultramicroscopy* **100**, 197–201 (2004).
12. C. K. Riener, F. Kienberger, C. D. Hahn, et al., *Analitica Chimica Acta* **497**, 101–114 (2003).
13. C. Reiner, C. Stroh, A. Ebner, et al., *Anal. Chim. Acta* **479**, 59–75 (2003).
14. A. Limanskii, *Tsitol. Genet.* **39** (2), 64–71 (2005).
15. A. Limansky, L. Shlyakhtenko, S. Schaus, et al., *Probe Microscopy* **2**, 227–234 (2002).
16. J. Cleveland, S. Manne, D. Bocek, and P. Hansma, *Rev. Sci. Instrum.* **64**, 403–405 (1993).
17. J. Hazel and V. Tsukruk, *Thin Solid Films* **339**, 249–257 (1999).
18. H. Butt, *Biophys. J.* **60**, 1438–1444 (1991).
19. M. Kitazawa and A. Toda, *Jpn. J. Appl. Phys.* **41**, 4928–4931 (2002).
20. M. Kitazawa, K. Shiotani, and A. Toda, *Jpn. J. Appl. Phys.* **42**, 4844–4847 (2003).
21. L. Shlyakhtenko, A. Gall, J. Weimer, et al., *Biophys. J.* **77**, 568–576 (1999).
22. A. Limanskii, *Biopolim. Kletka* **18**, 62–70 (2002).
23. A. Limanskii, *Usp. Sovrem. Biol.* **123**, 531–542 (2003).